



Supplementary Materials for

Progenitor Outgrowth from the Niche in *Drosophila* Trachea Is Guided by FGF from Decaying Branches

Feng Chen and Mark A. Krasnow*

*Corresponding author E-mail: krasnow@stanford.edu

Published 10 January 2014, *Science* **343**, 186 (2014)
DOI: 10.1126/science.1241442

This PDF file includes:

Materials and Methods
Figs. S1 to S10
Full Reference List
Captions for Movies S1 to S4

Other Supplementary Material for this manuscript includes the following:
(available at www.sciencemag.org/content/343/6167/186/suppl/DC1)

Movies S1 to S4

Supporting Online Material

Materials and methods

Drosophila strains and reporter lines

btl-RFP-moe (gift from M. Affolter, Biozentrum University of Basel) is a transgene that expresses an RFP-moesin fusion protein under the control of a *btl* enhancer element (15). Line CB02854 (25) (Flytrap, Yale University) contains a GFP enhancer trap insertion at the *btl* locus. The Gal4-UAS system (26) was used to express fluorescent reporters, other proteins, and RNAi transgenes in specific tissues and cell types *in vivo*. Gal4 drivers were: *ppk4-Gal4* (16) (gift from L. Liu, Peking University) a transgene containing 2 kb of the *ppk4* promoter region controlling *Gal4* and expressed in all larval tracheal cells; *esg^{P127}-Gal4* (11, 27, 28), an enhancer trap at the *escargot* locus expressed in all imaginal progenitor cells and tracheal fusion cells; *prd-Gal4* (29), a transgene expressing *Gal4* in the *paired* pair-rule gene pattern; and Gal4 enhancer trap lines NP2211 and NP3520 (Drosophila Genetic Resource Center; Kyoto Institute of Technology) (24) with insertions at the *btl* locus. UAS responders were: *UAS-GFP* (29), *UAS-FLP122* (29), *UAS-DN-btl* (19), *UAS-bnl-RNAi* GD5730 and *UAS-btl-RNAi* GD948 (30) (Vienna Drosophila RNAi Center), *UAS-bnl-A1-1* (31), and *UAS-rpr* (29). *tub-Gal80ts* (29), a transgene that ubiquitously expresses a temperature-sensitive conditional repressor of GAL4, was used to limit UAS responder expression to specific time periods. The FLP recombinase system (32) was used for permanent marking of tissues and cells and lineage labeling. *dfr-FLP* (M. Metzstein and M.A.K., unpublished) is a transgene with a multimerized tracheal-specific *dfr* enhancer element (33) cloned upstream of an *hsp70* minimal promoter driving expression of FLP. *act5c>Y>Gal4* (34), a ubiquitously expressed FLP-dependent transgene in which Gal4 is expressed following FLP-mediated recombination, was used for FLP-out experiments (see below). Crumbs::GFP (Crb::GFP-A) (gift from Y. Hong, University of Pittsburgh School of Medicine) encodes a functional Crumbs-GFP fusion protein knocked into the endogenous *crumbs* locus (35), which labels the apical epithelial surface and tracheal lumen. All crosses were carried out at 25°C unless otherwise indicated.

Lineage trace and FLP-out experiments

All lineage trace and FLP-out experiments used *act5c>Y>Gal4*, *UAS-GFP* and a *FLP* transgene. Expression of FLP recombinase catalyzes “FLP-out” (removal) of a stop cassette and thereby activation of the *act5c>Y>Gal4* transgene (34), which then expresses Gal4 that drives expression of *UAS-GFP*, to permanently label the cells in which recombination has occurred and their progeny, and expression of other UAS responders as indicated.

esg^{P127}-Gal4 (11, 27, 28) is expressed in imaginal cells, including the SB tracheal progenitors, and fusion cells of the tracheal system. FLP-out experiments with a *Drosophila* strain carrying *esg^{P127}-Gal4* and *UAS-FLP* transgenes crossed to the *act5c>Y>Gal4*, *UAS-GFP* strain permanently labels imaginal cells and their progeny (11). Larval tracheal cells were also sporadically labeled, but because rearing the animals at 18°C reduced this unwanted labeling, all crosses and FLP-out experiments with *esg^{P127}-Gal4* were conducted at 18°C.

drifter (*dfr*)/ *ventral veins lacking* (*vvl*) is a transcription factor expressed in tracheal cells during embryonic development (36). In *dfr-FLP*; *act5c>Y>Gal4*, *UAS-GFP* animals raised at 25°C, GFP was expressed in larval tracheal clones that covered approximately 30 to 80% of the trachea. Animals raised at lower temperature had larger clones. To knockdown *bnl* in tracheal clones that encompassed the full circumference of the DT, *dfr-FLP*/ *act5c>Y>Gal4*,

UAS-GFP; btl-RFP-moe/ UAS-bnl RNAi animals were raised at 21°C. *dfr-FLP/ act5c>Y>Gal4, UAS-GFP; btl-RFP-moe/ UAS-bnl* animals raised at 25°C expressing ectopic Bnl (*UAS-bnl-A1-1*) in tracheal clones were viable and survived beyond puparium formation; the animals had slight defects in the shape and spacing of the larval branches and had local tufts of tracheoles, but the overall structure of the larval tracheal system was unaffected (fig. S10).

FLP-out experiments with the *prd-Gal4* driver in *act5c>Y>Gal4, UAS-GFP/ UAS-FLP; prd-Gal4, btl-RFP-moe/ UAS-bnl RNAi* animals labeled alternating segments of the epidermis and predominantly labeled alternating segments of the trachea.

Larval and pupal staging

L2 larvae were distinguished from L3 larvae by appearance of anterior spiracles. The relative ages of L3 larvae were inferred from the size of the animal; older larvae are larger. Wandering third instar larvae (W3L) and newly formed pupae (0 hr APF) were identified as described (37). 0 hr APF animals were selected and subsequent time points were determined by hours elapsed since selection.

Antibody and tracheal stains

Larvae and pupae were dissected by ventral filleting and fixed in 4% paraformaldehyde for 30 minutes then immunostained as described (38). GFP and RFP signals were amplified by immunostaining with polyclonal chicken anti-GFP (Abcam, ab13970; used at 1:1000) and polyclonal rabbit anti-DsRED (Clontech #632496; 1:300) primary antibodies. Pruned (dSRF) protein was detected with mAb2-161, a monoclonal mouse anti-dSRF antibody (used at 1:200) (39). A monoclonal rabbit anti-cleaved Caspase-3 antibody (Cell Signaling #9664) was used to detect apoptotic cells. Secondary antibodies used were: DyLight649-conjugated donkey-anti-chicken, DyLight649-conjugated donkey-anti-rabbit, Cy5-conjugated goat-anti-mouse (Jackson ImmunoResearch), Alexa488-conjugated goat-anti-chicken and Alexa555-conjugated goat-anti-rabbit (Invitrogen). Tracheal lumens were stained with Alexa Fluor 350-conjugated or tetramethylrhodamine-conjugated wheat germ agglutinin (WGA) (Invitrogen; 1:1000) and with a rhodamine-conjugated chitin-binding probe (NEB; 1:300) for 1 hour at room temperature. Nuclei were stained with 4',6-Diamidino-2-Phenylindole, Dihydrochloride (DAPI) (Molecular Probes). Cuticle that lines larval tracheae autofluoresces and was also detected in the DAPI channel. Specimens were analyzed and digital images captured on confocal (Leica SP2 AOBS) and conventional fluorescence (Zeiss AxioPhot and Leica MZ16 FA) microscopes. Air-filled tracheae were visualized on the Leica SP2 AOBS by reflected light. Unless otherwise indicated, all fluorescent micrographs are maximum projections of the confocal stack.

Live imaging progenitor migration

Immobile white *btl-RFP-moe* pupae (0 hr APF) were cleaned with a damp tissue and placed within a drop of halocarbon oil on a 6 cm Petri dish. Pupae were positioned with forceps for optimal imaging of tracheal progenitors in Tr4 and Tr5. Movies were acquired on a Zeiss Axio Observer.Z1 inverted microscope equipped with a XL multi S1 incubator to maintain temperature at 25°C. Images were acquired every 3 - 5 minutes for up to 7 hours, after which the RFP signal from the *btl-RFP-moe* reporter diminishes. Image capture times were limited to 0.5 sec or less to minimize phototoxicity.

Monitoring *bnl* expression with *bnl* reporter lines

Because it proved difficult to obtain reliable signals for *bnl* expression by *in situ* hybridization or immunostaining for Bnl protein during metamorphosis, we used Gal4 enhancer trap lines NP2211 and NP3520 and GFP enhancer trap line CB02854 with insertions at the *bnl* locus within a 300 bp region 5' to the *bnl* transcription start site to monitor *bnl* expression during metamorphosis. All three enhancer trap reporters showed dynamic expression all along the route of PAT progenitor migration, with the exception noted below. CB02854 reported slightly earlier expression along the DT than NP2211 and NP3520, presumably because the binary Gal4/UAS system introduces a delay due to translation of Gal4 and induction of the GFP reporter. No expression of these reporters was detected in the section of DT between the Tr4 and Tr5 TC branches (the Tr5 DT), along which the Tr4 SB progenitors migrate to reach the next section of DT where they meet the progenitors from the Tr5 SB and continue migrating posteriorly along the DT. We infer that this part of the endogenous *bnl* expression pattern has a separate enhancer not reported by these enhancer trap lines because *bnl* RNAi knockdown in this region blocked Tr4 progenitor migration (fig. S7D; Movie S4).

Supplementary Figures

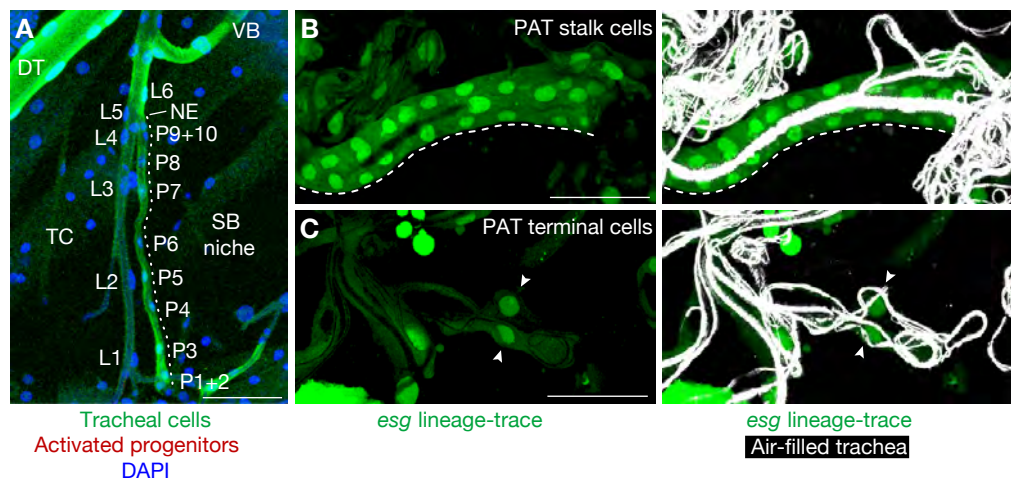


Figure S1. Visualizing and lineage-tracing tracheal progenitors that migrate out of the spiracular branch niche. (A) Cells in the Tr5 spiracular branch (SB) niche (dotted line) before progenitor activation. A portion of tracheal metamere Tr5 is shown from a *ppk4>GFP; btl-RFP-moe* second instar larva (L2) stained for GFP to show tracheal cells (green), for RFP to show activated progenitors (red), and labeled with DAPI to show cell nuclei (blue). The 10 progenitor cells (P1 - P10) in the spiracular branch (SB) niche are labeled, as are six larval tracheal cells (L1-L6) in the neighboring transverse connective (TC). Progenitors P9 and P10 connect to L5 and L6 and the rest of the larval tracheal system at the SB-TC junction, which we refer to as the niche exit (NE) and indicate with a dash. P1 and P2 connect to the epidermis. Progenitors in tracheal metameres Tr2 - Tr4 and Tr6 - Tr9 (not shown) appear similar. DT, dorsal trunk; VB, visceral branch. (B, C) *escargot>FLP* lineage trace showing imaginal progenitors give rise to pupal abdominal trachea (PAT). Fluorescent micrographs of differentiated PAT stalk (B) and terminal (C) cells in an *esg^{P127}-Gal4, UAS-GFP/act5c>Y>Gal4, UAS-GFP; UAS-FLP* pupa approximately 24 hr after puparium formation (APF) at 18°C. SB and other *esg^{P127}*-lineage (imaginal) progenitors and their descendants are labeled with GFP (green), and air-filled tracheae and terminal branches (tracheoles) are visualized by reflected light (white). Dashed line, PAT stalk; arrowheads, individual terminal cells, each of which has formed many tracheoles. Bars, 50 μ m.

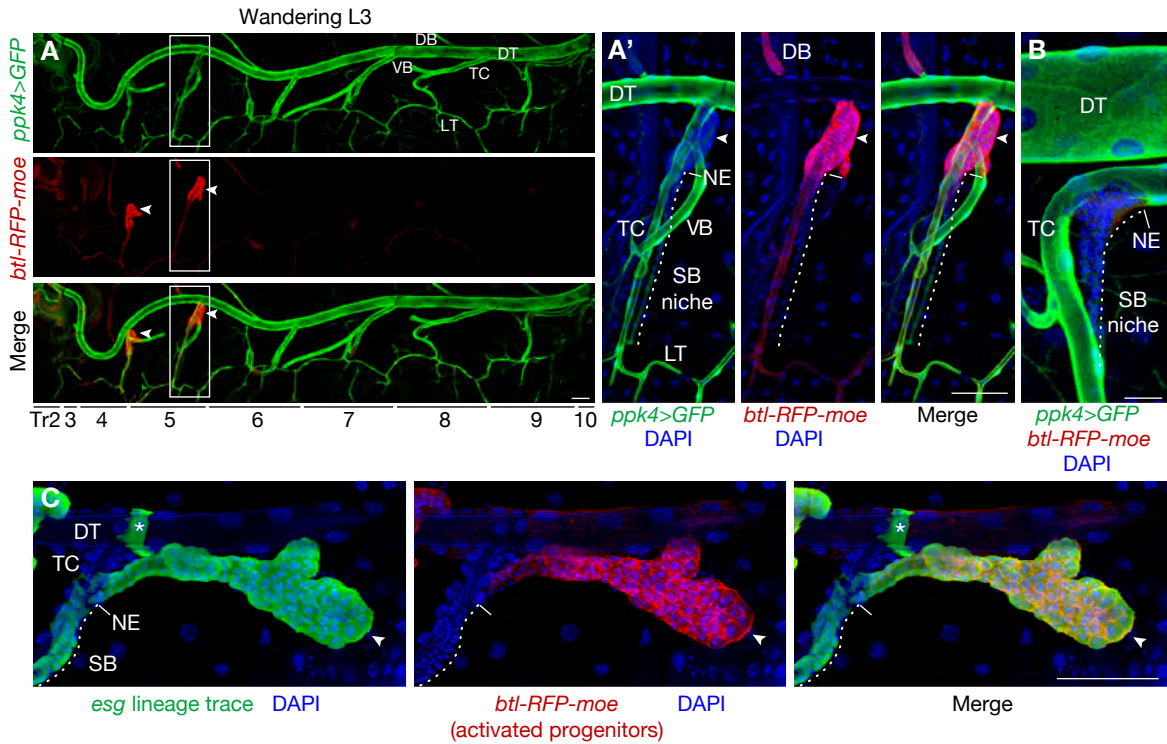


Figure S2. Selective expression of a *breathless* FGFR reporter in outgrowing progenitors. (A) Fluorescent micrograph of a *ppk4>GFP*; *btl-RFP-moe* wandering third instar (W3L) larva stained for GFP to show *ppk4>GFP* expression and for RFP to show *btl-RFP-moe* expression as in Fig. 1E. Close-ups of metamere Tr5 (boxed) are shown in A', with nuclei stained with DAPI (blue). Note that larval tracheal cells along the dorsal trunk (DT), transverse connectives (TC), lateral trunk (LT), visceral branch (VB) and posterior (Tr6 to Tr10) dorsal branches (DB) express *ppk4>GFP* but little or no *btl-RFP-moe*, which must have been downregulated after embryonic development (15). Conversely, progenitors have turned off the *ppk4>GFP* reporter, and Tr4 and Tr5 progenitors that are exiting the niche (arrowheads) highly express the *btl* reporter. Dotted lines, SB niche. Dashes, SB niche exit (NE). De-differentiating cells in anterior (Tr2 to Tr5) dorsal branches (DB) (11) also express the *btl-RFP-moe* reporter (A') though at lower levels. (B) Posterior SB niche after progenitor activation. A portion of tracheal metamere Tr9 of the larva in A is shown with nuclei stained with DAPI (blue). Progenitors have proliferated and those near the niche exit express low but detectable *btl-RFP-moe* (red). However, progenitors do not exit the niche, as they do in Tr4 and Tr5. (C) Close up of progenitors growing out of the SB niche in an *esg*^{P127}-*Gal4*, *UAS-GFP/act5c>Y>Gal4*, *UAS-GFP*; *UAS-FLP/btl-RFP-moe* pupa 6 hr APF at 18°C stained for *esg*^{P127} lineage-trace progenitors (anti-GFP, green), activated progenitors (anti-RFP, red), and nuclei (DAPI, blue). Note that all progenitors that have exited the SB niche (arrowheads) express the *btl* reporter but those still in the niche (dotted line) do not. *, larval fusion cells that also express *esg*. Dash, SB niche exit (NE). Bars, 100 μm (A, C) and 25 μm (B).

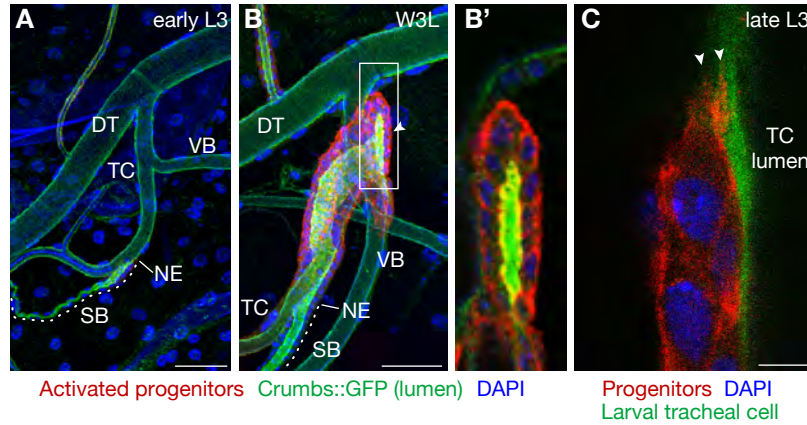


Figure S3. Progenitor outgrowth morphology. Portion of tracheal metamere Tr4 in *btl-RFP-moe/crumbs::GFP* early third-instar (L3) (A) and wandering third instar (W3L) (B) larvae stained for activated tracheal progenitors (anti-RFP, red) and apical tracheal surface and lumen (anti-GFP, green). In early L3 larvae (A), the SB contains a lumen and forms a junction with the larval transverse connective (TC) at the niche exit (NE) site. In wandering L3 larvae (B), the outgrowing progenitors have formed a monolayer-epithelial sac extending from the SB niche (arrowhead). The lumen of the expanding progenitor sac is continuous with the SB lumen and larval TC at the NE. Inset (B') shows an optical z-section of the boxed region. Note Crumbs::GFP and RFP-moesin co-localization on apical progenitor cell surfaces. (C) Close-up of migrating progenitors in Fig. 1D. Progenitors migrate on the basal surface of larval tracheal cells; cytoplasmic extensions emanate from the leading progenitors (arrowheads), indicating active migration. Bars, 50 μm (A, B) and 5 μm (C).

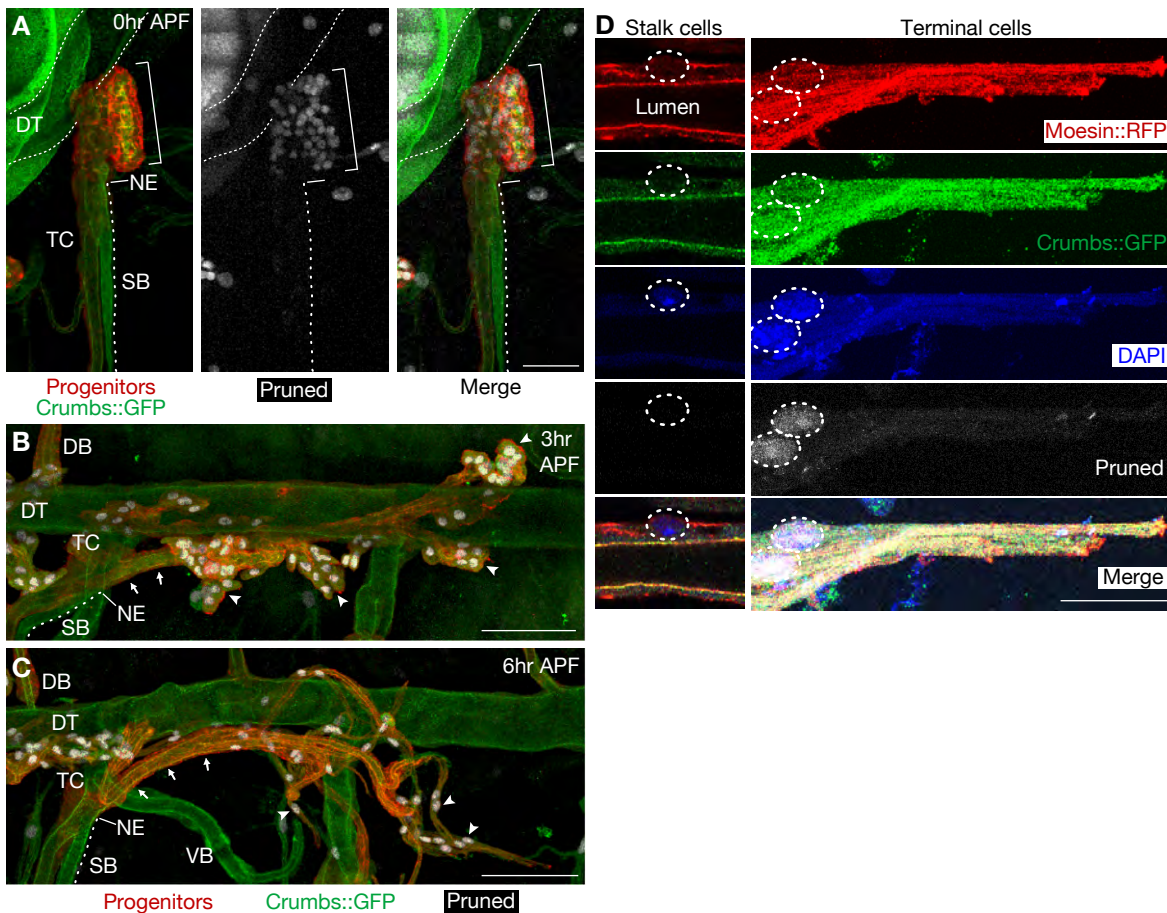


Figure S4. Migrating progenitors initiate the tracheal morphogenesis program. (A) Portion of tracheal metamere Tr5 in *bitl-RFP-moe/crumbs::GFP* larva at onset of puparium formation (0 hr APF) stained for Pruned SRF (white), tracheal progenitors (anti-RFP, red), and apical surfaces of tracheae (anti-GFP, green). Note that a subset of progenitors in the outgrowing cluster (bracket) has initiated the terminal cell differentiation program as indicated by expression of Pruned. Dotted line, SB niche; dash, SB niche exit (NE). (B, C) Pupae as above at 3 hr (B) and 6 hr (C) APF. Pruned-expressing progenitors are segregated at the tips of the outgrowing PAT (arrowheads), while Pruned-negative cells form the PAT stalk (arrows). (D) Close-up of PAT stalk and terminal cells of the pupa in C also stained for DAPI to show nuclei. Note terminal cells have elongated morphology and have formed intracellular lumens (tracheoles) (outlined by RFP-moesin and Crumbs::GFP) whereas progenitors in the stalk do not express Pruned, do not form tracheoles, and have apical Crumbs::GFP localization. Bars, 50 μm (A), 100 μm (B, C), 25 μm (D).

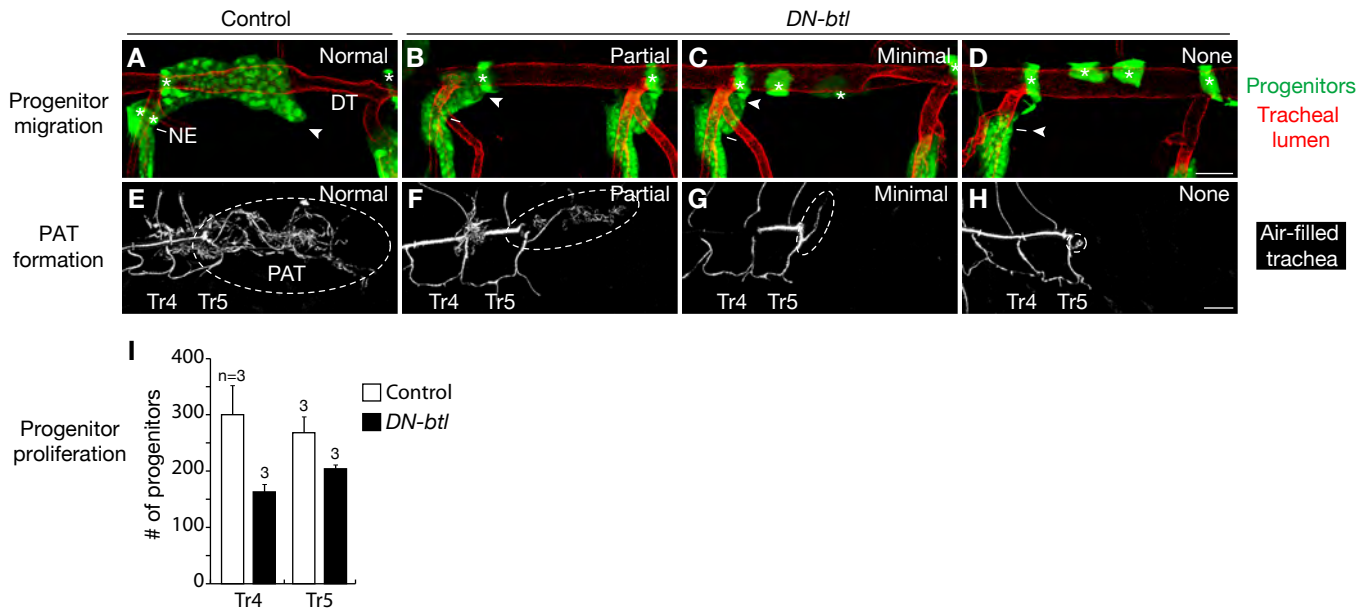


Figure S5. Effect of dominant negative *Breathless* on progenitor migration, proliferation, and PAT formation.

Dominant-negative *breathless* (*DN-btl*) was expressed in SB tracheal progenitors and their progeny, and the animals were analyzed 6 hr APF at 18°C for effects on Tr4 and Tr5 progenitor migration (A-D) as described in Fig. 2A, or for effects on progenitor proliferation by counting the number of progenitors (I), or animals were reared for an additional 1 to 2 days to allow PAT formation (E-H). (A-D) Examples of progenitor migration phenotypes. (A) Normal (Class 0), migration similar to that in control pupae. (B) Partial (Class I), reduced migration along DT. (C) Minimal (Class II), no migration along DT. (D) None (Class III), progenitors do not exit SB niche. Progenitors, green (GFP fluorescence); larval tracheal branches, red (rhodamine-conjugated WGA and rhodamine-conjugated chitin-binding protein); dash, niche exit (NE); *, larval tracheal fusion cells and sporadic larval tracheal cells that also express the progenitor lineage label. (E-H) Examples of PAT formation phenotypes. (E) Normal, extensive PAT formation similar to that in controls. (F) Partial, reduced PAT ramification and extension into posterior. (G) Minimal, limited PAT formation and extension with thin branches at PAT base. (H) None, no PAT formation. White, mature air-filled pupal tracheae; dashed ovals, extent of PAT formation. Similar though less severe progenitor migration and PAT formation phenotypes were observed with expression of a *btl RNAi* transgene. (I) Quantification of cell number in Tr4 and Tr5 SB niches. The 10 SB progenitors (fig. S1A) proliferate extensively in both control and *DN-btl*-expressing pupae, but note there are fewer cells in the *DN-btl* pupae, in which progenitors do not leave the niche. Bars, 50 μm (A-D), 100 μm (E-H).

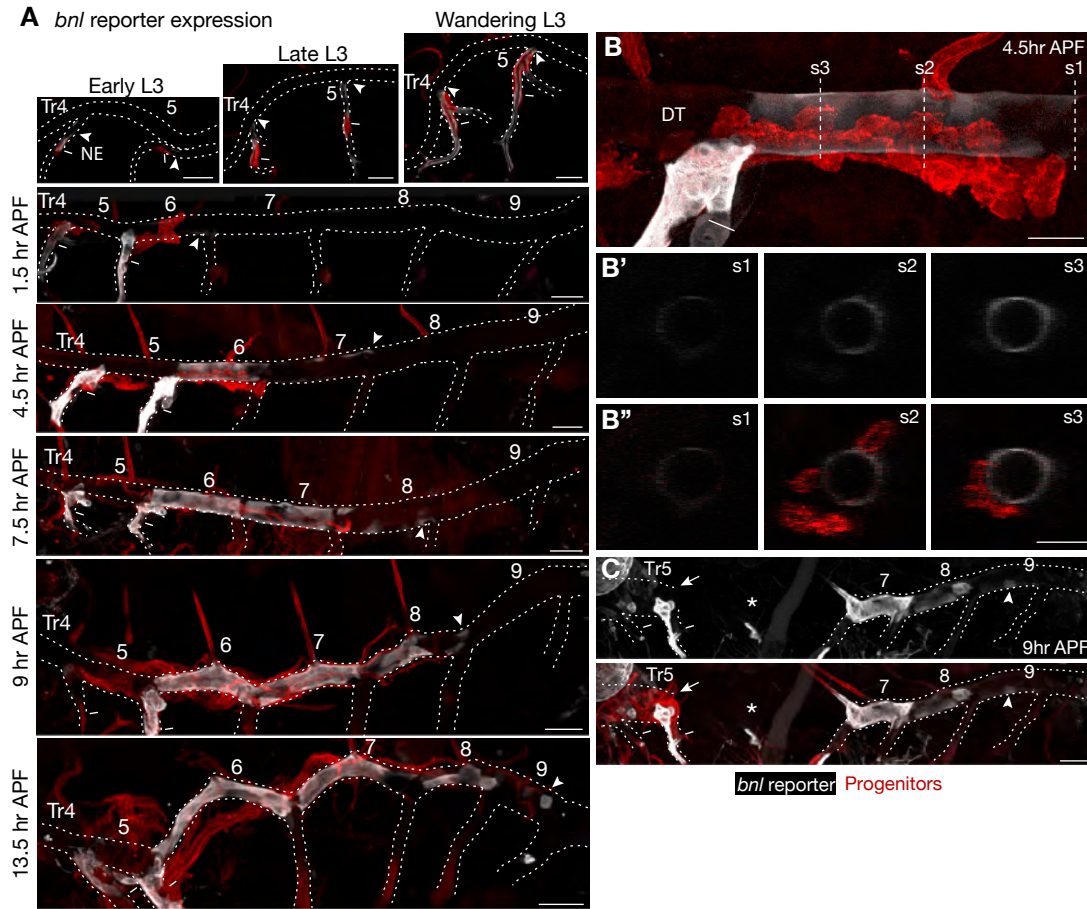


Figure S6. Expression of *branchless* (*bnl*) just ahead of migrating tracheal progenitors. (A) *bnl-Gal4 NP2211/UAS-GFP; btl-RFP-moe* animals of the indicated ages showing *bnl* reporter expression (GFP immunostain, white) as in Fig. 3A but co-stained to show relationship to migrating progenitors (RFP immunostain, red). Isolated larval cells initiate *bnl* reporter expression (arrowheads) ahead of migrating progenitors. Note reporter expression in TC cells ventral to the niche exit that is ignored by migrating progenitors, and absence of reporter expression in the Tr5 DT, along which Tr4 progenitors migrate to meet Tr5 progenitors. Dashes, niche exit (NE). (B) Close up of Tr6 in pupa 4.5 hr APF. Optical sections through dorsal trunk (DT) at planes indicated (s1, s2, s3) are shown in B' and B'' (*bnl* reporter expression, white; migrating progenitors, red). Although *bnl* reporter expression initially appears in individual DT cells (section s1), it expands to cover the entire circumference of the DT (section s3). However, progenitors do not completely envelop the entire circumference (section s3). (C) A 9 hr APF pupa, stained as above, with sporadic break that has separated DT into anterior and posterior regions. Note that progenitors (red, arrow) have not migrated beyond the lesion (*) but *bnl* reporter expression has expanded beyond lesion into posterior metameres (arrowhead) just as in animals with intact DT (panel A). Bars, 100 μ m (A,C), 50 μ m (B).

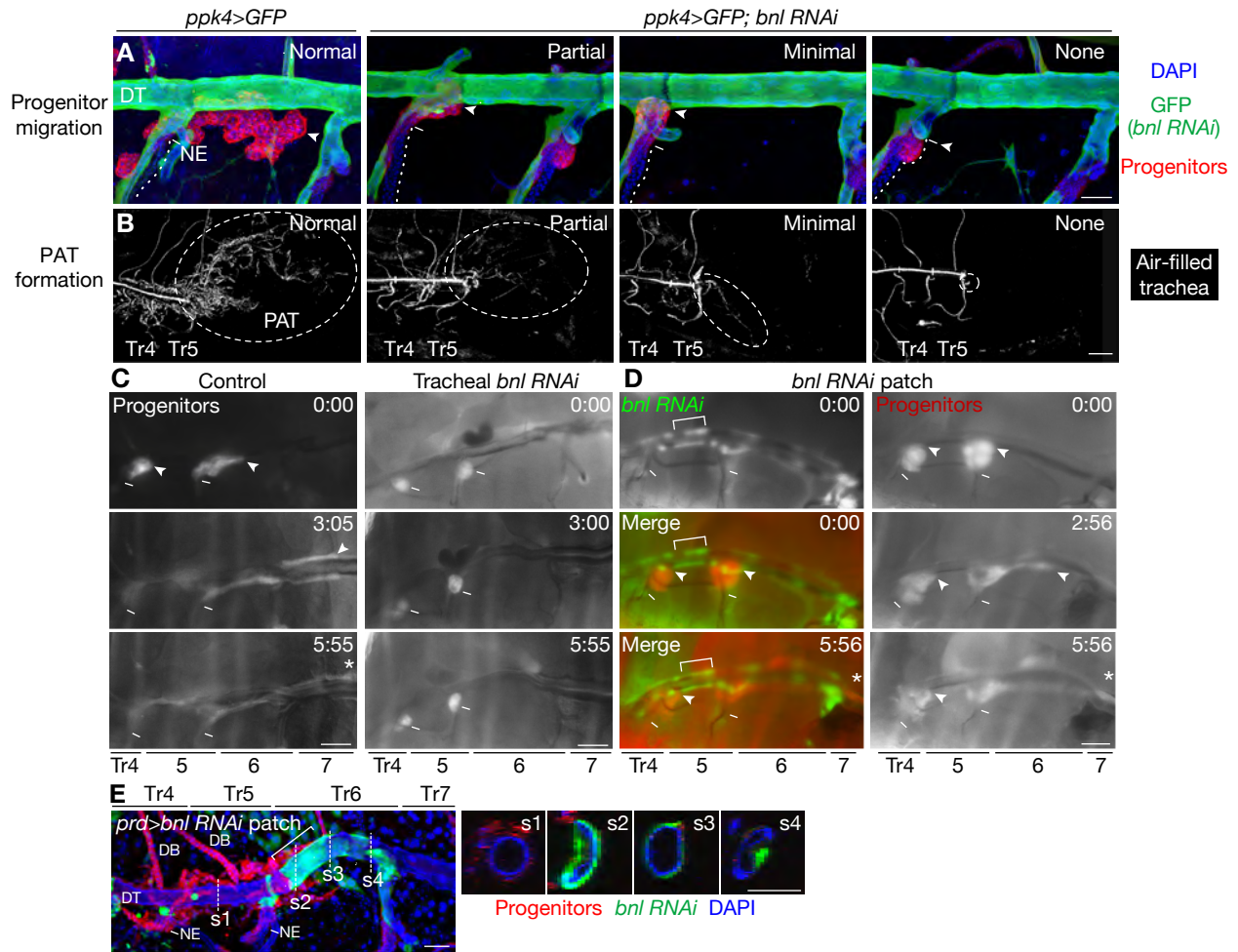


Figure S7. Progenitor migration and PAT formation phenotypes from *branchless* (*bnl*) knockdown along migration route. (A) Progenitor migration in a control (*ppk4-Gal4/ UAS-GFP; btl-RFP-moe*) and *ppk4-Gal4/ UAS-GFP; btl-RFP-moe/ UAS-bnl RNAi* pupa in which *bnl RNAi* was expressed in all larval tracheal cells. The effect on progenitor migration 3 hr APF was analyzed as described in Fig. 2A after staining for progenitors (anti-RFP, red), larval tracheal cells in which *bnl* is knocked down by RNAi (anti-GFP, green), and nuclei (DAPI, blue). Examples of migration phenotypes are indicated, classified as in fig. S5A-D. Dotted line, SB niche; dash, niche exit (NE); arrowheads, extent of progenitor migration. (B) Pupae as in A reared for another 1 to 2 days to allow PAT formation. Air-filled trachea, visualized by reflected light (white). Dashed circles, extent of PAT formation. Examples of PAT formation phenotypes are indicated, classified as in fig. S5E-H. (C) Frames from live imaging (see also Movie S2) at the indicated times APF of control and tracheal *bnl RNAi* knockdown pupae as in A. Progenitors (white, *btl-RFP-moe*) migrate along larval DT in control pupa, but they never leave the SB niche (dash) in the tracheal *bnl* knockdown pupa. Arrowheads, progenitor migration front; *, progenitor migration extends beyond field of view. (D) Frames from live imaging (see Movie S4) at the indicated times APF of a *dfr-FLP/ act5c>Y>Gal4, UAS-GFP; btl-RFP-moe/ UAS-bnl RNAi* pupa in which *bnl* expression was knocked down in a DT patch along the Tr5 DT (bracket). Tr4 progenitors are stalled next to the large patch, whereas Tr5 progenitors are not stalled by the smaller patches of *bnl RNAi* expression in the Tr6 DT. (E) Confocal fluorescent micrograph of a *UAS-FLP/ act5c>Y>Gal4, UAS-GFP; prd-Gal4, btl-RFP-moe/ UAS-bnl RNAi* pupa fixed following 6 hours of live-imaging (see Fig. 3D and Movie S3) and then stained for tracheal progenitors (anti-RFP, red), cells expressing *bnl RNAi* (anti-GFP, green), and nuclei (DAPI, blue). Optical sections at the planes indicated (s1 - s4) are shown. Progenitors stalled next to the short segment of DT, approximately 2 to 3 larval cells wide, in which *paired* FLP-out drives a patch of expression (bracket) of *UAS-bnl RNAi* and *UAS-GFP*. Optical sections show that *bnl RNAi* expressing cells encompass full circumference of DT. Bars, 50 μ m (A and E), 100 μ m (B-D).

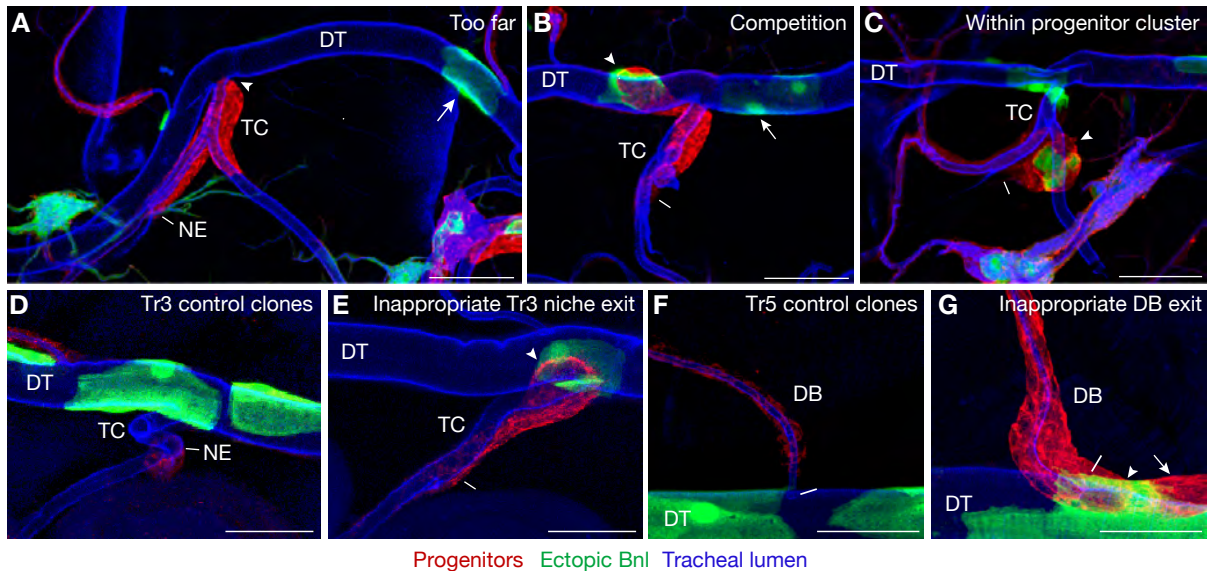


Figure S8. Examples of *branchless*-expressing clones that did not induce ectopic migration of PAT progenitors and clones that induced migration of progenitors that do not normally migrate. GFP-labeled clones of *bnl*-expressing cells (green) were induced and analyzed in wandering third-instar larvae as in Figure 4. Dash, niche exit (NE); DT, dorsal trunk; TC, transverse connective; DB, dorsal branch; arrowheads, progenitor migration front. (A) A clone (arrow) far from the Tr4 migrating progenitors (red) that did not induce ectopic progenitor migration. (B) A pair of clones (arrow and arrowhead) in which Tr5 progenitors have migrated toward only one of the clones (arrowhead). (C) A clone in the Tr5 progenitor cell cluster. Migration is disrupted and progenitors remain near the SB niche. (D) Control clones in Tr3. Tr3 progenitors normally remain within the SB niche during PAT outgrowth and are unaffected by control clones expressing only GFP. (E) A *bnl*-expressing clone that has recruited Tr3 progenitors out of the niche to DT. Note that the Tr3 progenitors have reached the DT clone even though there is no endogenous (or ectopic) *bnl* expression in the TC, perhaps because the Tr3 TC is shorter than those in other metameres. (F) Control clone near Tr5 DB. Progenitors in anterior DBs (Tr2 to Tr5) derived from de-differentiated larval cells express *btl-RFP-moe* (fig. S2A) and proliferate but normally remain in the DB niche (see also fig. S2A' and fig. S4B, C). (G) Tr5 DB progenitors (arrowhead) are sometimes recruited onto the DT by clones expressing ectopic *bnl*. Arrow, Tr5 SB progenitors also recruited by the clone. Dash, DB boundary at DB/DT junction. Bars, 100 μ m (A-C), 50 μ m (D-G).

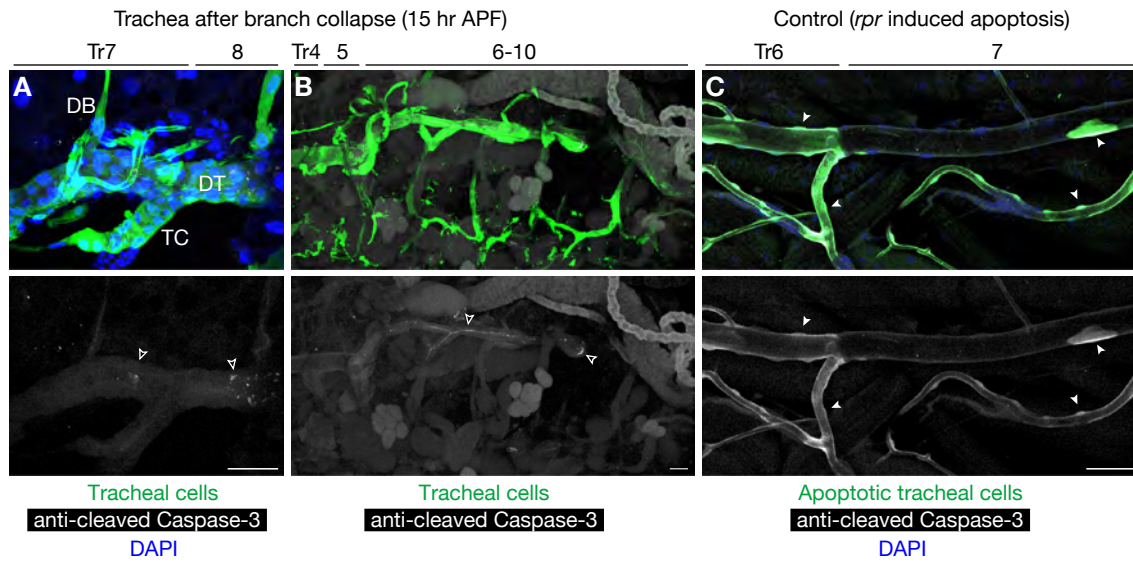


Figure S9. Decaying tracheal branches do not express cleaved Caspase-3. (A, B) Fluorescent micrographs of *ppk4>GFP; btl-RFP-moe* 15 hr APF pupae immunostained for cleaved Caspase-3 (white), a marker of apoptosis, and for GFP (green) to show tracheal cells. Nuclei are stained with DAPI (blue). Larval tracheal cells in posterior metameres (Tr6 to Tr10) are lost during metamorphosis (10) but are not stained by the cleaved Caspase-3 immunostain, suggesting that they die later in metamorphosis or by other mechanisms. Thin or spotty staining (open arrowheads) is antibody trapped in collapsed posterior tracheal branches (Fig. 1). (C) Fluorescent micrograph of a *ppk4-Gal4, UAS-GFP/ UAS-rpr; tub-Gal80ts/ +* wandering third-instar larva stained as in A and B as a control to show cleaved Caspase-3 expression in apoptotic tracheal cells. Note cleaved Caspase-3 immunostaining (white) in tracheal cells activating expression of the apoptosis inducer *reaper* (*rpr*) and marked by GFP (green; arrowheads). Animals were raised at the permissive temperature (18°C) of the GAL80ts repressor to prevent early ectopic *rpr* expression and allow embryonic tracheal formation, and then transferred to the non-permissive temperature (30°C) to activate *rpr*-induced apoptosis. Bars, 50 µm.

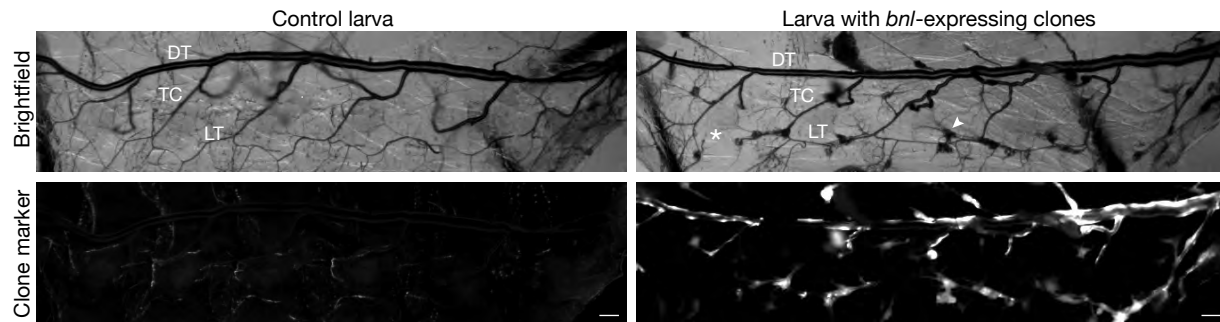


Figure S10. Effect on the larval tracheal system of tracheal clones expressing *branchless* FGF. Brightfield (upper) and fluorescence (lower) images of a control *Cyo/ act5c>Y>Gal4, UAS-GFP; btl-RFP-moe/ UAS-bnl* wandering third instar larva and a *dfr-FLP/ act5c>Y>Gal4, UAS-GFP; btl-RFP-moe/ UAS-bnl* larva in which the GFP-marked clones express ectopic *bnl*. Note tracheal patterning in the larva with *bnl*-expressing clones was not globally perturbed, although there are local defects including a sporadic gap (*) in the lateral trunk (LT) and scattered foci of densely-packed tracheoles (arrowhead). DT, dorsal trunk; TC, transverse connective. Bars, 100 μ m.

1241442s1.mov

Movie S1. Tracheal progenitors migrating along the larval dorsal trunk.

Fluorescence imaging of a live *btl-RFP-moe* white pupa beginning just after puparium formation (0 hr APF) in which migrating PAT progenitors originating from tracheal metameres Tr4 and Tr5 and expressing RFP-moesin (white; arrowheads) were visualized through the cuticle. Images were acquired every three minutes for seven hours at 25°C. DT, dorsal trunk; TC, transverse connective; dash, SB niche exit. Progenitors move toward the posterior at ~1.7 µm/min, maintaining a close association with the DT and crawling and wrapping around it as they migrate. Tr4 progenitors move onto DT about one hour later than Tr5 progenitors. Note multiple tips of migrating progenitors, each taking slightly different paths along DT into posterior. Bar, 100 µm.

1241442s2.mov

Movie S2. Effect of *branchless* knockdown on progenitors exiting SB niche.

Fluorescence imaging of a live *ppk4-Gal4/ UAS-GFP; btl-RFP-moe/ UAS-bnl RNAi* pupa in which *bnl* was knocked down by RNAi in larval tracheal cells (marked by GFP, pseudo-colored green in merged images). Tracheal progenitors marked by RFP fluorescence and pseudo-colored red in merged images (arrowheads) do not move beyond niche exit (dash). DT, dorsal trunk; TC, transverse connective. Images were acquired every five minutes from 0 hr to 6 hr APF at 25°C. Bar, 100 µm.

1241442s3.mov

Movie S3. Effect of *branchless* knockdown in patch along Tr5 progenitor migration route.

Live imaging of an *act5c>Y>Gal4, UAS-GFP/ UAS-FLP; prd-Gal4, btl-RFP-moe/ UAS-bnl RNAi* pupa in which *bnl* expression was inactivated in portion of Tr6 DT (bracket) by expression of *bnl RNAi* mediated by *paired-Gal4*. Tr5 tracheal progenitors move onto DT but stall when they reach DT patch where *bnl RNAi* is expressed; meanwhile, Tr4 progenitors progress posteriorly. DT, dorsal trunk; TC, transverse connective; dash, SB niche exit; arrowhead, progenitors. Images were acquired every five minutes from 0 hr to 6 hr APF at 25°C. Bar, 100 µm.

1241442s4.mov

Movie S4. Effect of *branchless* knockdown in patch along Tr4 progenitor migration route.

Live imaging of a *dfr-flp / act5c>Y>Gal4, UAS-GFP; btl-RFP-moe/ UAS-bnl RNAi* pupa in which *bnl* expression was inactivated in a portion of Tr5 DT (bracket) by expression of *bnl RNAi*. Tr4 tracheal progenitors stall next to DT patch where *bnl RNAi* is expressed. DT, dorsal trunk; TC, transverse connective; dash, SB niche exit; arrowhead, progenitors. Images were acquired every five minutes from 0 hr to 6 hr APF at 25°C. Bar, 100 µm.

References and Notes

1. N. Barker, S. Bartfeld, H. Clevers, Tissue-resident adult stem cell populations of rapidly self-renewing organs. *Cell Stem Cell* **7**, 656–670 (2010). [Medline](#) [doi:10.1016/j.stem.2010.11.016](https://doi.org/10.1016/j.stem.2010.11.016)
2. G. B. Adams, D. T. Scadden, The hematopoietic stem cell in its place. *Nat. Immunol.* **7**, 333–337 (2006). [Medline](#) [doi:10.1038/ni1331](https://doi.org/10.1038/ni1331)
3. A. Alvarez-Buylla, D. A. Lim, For the long run: Maintaining germinal niches in the adult brain. *Neuron* **41**, 683–686 (2004). [Medline](#) [doi:10.1016/S0896-6273\(04\)00111-4](https://doi.org/10.1016/S0896-6273(04)00111-4)
4. C. Blanpain, E. Fuchs, Epidermal homeostasis: A balancing act of stem cells in the skin. *Nat. Rev. Mol. Cell Biol.* **10**, 207–217 (2009). [Medline](#) [doi:10.1038/nrm2636](https://doi.org/10.1038/nrm2636)
5. E. Sancho, E. Battle, H. Clevers, Live and let die in the intestinal epithelium. *Curr. Opin. Cell Biol.* **15**, 763–770 (2003). [Medline](#) [doi:10.1016/j.ceb.2003.10.012](https://doi.org/10.1016/j.ceb.2003.10.012)
6. G. L. Ming, H. Song, Adult neurogenesis in the mammalian brain: Significant answers and significant questions. *Neuron* **70**, 687–702 (2011). [Medline](#) [doi:10.1016/j.neuron.2011.05.001](https://doi.org/10.1016/j.neuron.2011.05.001)
7. E. Nacu, E. M. Tanaka, Limb regeneration: A new development? *Annu. Rev. Cell Dev. Biol.* **27**, 409–440 (2011). [Medline](#) [doi:10.1146/annurev-cellbio-092910-154115](https://doi.org/10.1146/annurev-cellbio-092910-154115)
8. K. D. Poss, Advances in understanding tissue regenerative capacity and mechanisms in animals. *Nat. Rev. Genet.* **11**, 710–722 (2010). [Medline](#) [doi:10.1038/nrg2879](https://doi.org/10.1038/nrg2879)
9. T. Matsuno, Morphogenesis of pupal abdominal tracheae in a fruit fly, *Drosophila melanogaster*. *Jap. J. Appl. Entomol. Zool.* **34**, 165–167 (1990). [doi:10.1303/jjaez.34.165](https://doi.org/10.1303/jjaez.34.165)
10. G. Manning, M. A. Krasnow, in *The Development of Drosophila melanogaster*, M. Bate, A. Martinez-Arias, Eds. (Cold Spring Harbor Laboratory Press, Woodbury, NY, 1993), vol. 1, pp. 609–685.
11. M. Weaver, M. A. Krasnow, Dual origin of tissue-specific progenitor cells in *Drosophila* tracheal remodeling. *Science* **321**, 1496–1499 (2008). [doi:10.1126/science.1158712](https://doi.org/10.1126/science.1158712)
12. A. Guha, L. Lin, T. B. Kornberg, Organ renewal and cell divisions by differentiated cells in *Drosophila*. *Proc. Natl. Acad. Sci. U.S.A.* **105**, 10832–10836 (2008). [Medline](#) [doi:10.1073/pnas.0805111105](https://doi.org/10.1073/pnas.0805111105)
13. C. Pitsouli, N. Perrimon, Embryonic multipotent progenitors remodel the *Drosophila* airways during metamorphosis. *Development* **137**, 3615–3624 (2010). [Medline](#) [doi:10.1242/dev.056408](https://doi.org/10.1242/dev.056408)
14. M. Sato, Y. Kitada, T. Tabata, Larval cells become imaginal cells under the control of homothorax prior to metamorphosis in the *Drosophila* tracheal system. *Dev. Biol.* **318**, 247–257 (2008). [Medline](#) [doi:10.1016/j.ydbio.2008.03.025](https://doi.org/10.1016/j.ydbio.2008.03.025)
15. C. Ribeiro, M. Neumann, M. Affolter, Genetic control of cell intercalation during tracheal morphogenesis in *Drosophila*. *Curr. Biol.* **14**, 2197–2207 (2004). [Medline](#) [doi:10.1016/j.cub.2004.11.056](https://doi.org/10.1016/j.cub.2004.11.056)

16. L. Liu, W. A. Johnson, M. J. Welsh, *Drosophila* DEG/ENaC pickpocket genes are expressed in the tracheal system, where they may be involved in liquid clearance. *Proc. Natl. Acad. Sci. U.S.A.* **100**, 2128–2133 (2003). [Medline doi:10.1073/pnas.252785099](#)
17. K. Guillemin, J. Groppe, K. Ducker, R. Treisman, E. Hafen, M. Affolter, M. A. Krasnow, The *pruned* gene encodes the *Drosophila* serum response factor and regulates cytoplasmic outgrowth during terminal branching of the tracheal system. *Development* **122**, 1353–1362 (1996). [Medline](#)
18. C. Klämbt, L. Glazer, B. Z. Shilo, Breathless, a *Drosophila* FGF receptor homolog, is essential for migration of tracheal and specific midline glial cells. *Genes Dev.* **6**, 1668–1678 (1992). [Medline doi:10.1101/gad.6.9.1668](#)
19. M. Reichman-Fried, B. Z. Shilo, Breathless, a *Drosophila* FGF receptor homolog, is required for the onset of tracheal cell migration and tracheole formation. *Mech. Dev.* **52**, 265–273 (1995). [Medline doi:10.1016/0925-4773\(95\)00407-R](#)
20. D. Sutherland, C. Samakovlis, M. A. Krasnow, *branchless* encodes a *Drosophila* FGF homolog that controls tracheal cell migration and the pattern of branching. *Cell* **87**, 1091–1101 (1996). [Medline doi:10.1016/S0092-8674\(00\)81803-6](#)
21. J. Jarecki, E. Johnson, M. A. Krasnow, Oxygen regulation of airway branching in *Drosophila* is mediated by *branchless* FGF. *Cell* **99**, 211–220 (1999). [Medline doi:10.1016/S0092-8674\(00\)81652-9](#)
22. M. Sato, T. B. Kornberg, FGF is an essential mitogen and chemoattractant for the air sacs of the *Drosophila* tracheal system. *Dev. Cell* **3**, 195–207 (2002). [Medline doi:10.1016/S1534-5807\(02\)00202-2](#)
23. Materials and methods are available as supporting material on *Science* Online.
24. S. Hayashi, K. Ito, Y. Sado, M. Taniguchi, A. Akimoto, H. Takeuchi, T. Aigaki, F. Matsuzaki, H. Nakagoshi, T. Tanimura, R. Ueda, T. Uemura, M. Yoshihara, S. Goto, GETDB, a database compiling expression patterns and molecular locations of a collection of Gal4 enhancer traps. *Genesis* **34**, 58–61 (2002). [Medline doi:10.1002/gene.10137](#)
25. M. Buszczak, S. Paterno, D. Lighthouse, J. Bachman, J. Planck, S. Owen, A. D. Skora, T. G. Nystul, B. Ohlstein, A. Allen, J. E. Wilhelm, T. D. Murphy, R. W. Levis, E. Matunis, N. Srivali, R. A. Hoskins, A. C. Spradling, The Carnegie protein trap library: A versatile tool for *Drosophila* developmental studies. *Genetics* **175**, 1505–1531 (2007). [Medline doi:10.1534/genetics.106.065961](#)
26. A. H. Brand, N. Perrimon, Targeted gene expression as a means of altering cell fates and generating dominant phenotypes. *Development* **118**, 401–415 (1993). [Medline](#)
27. P. Steneberg, C. Englund, J. Kronhamn, T. A. Weaver, C. Samakovlis, Translational readthrough in the *hdc* mRNA generates a novel branching inhibitor in the *Drosophila* trachea. *Genes Dev.* **12**, 956–967 (1998). [Medline doi:10.1101/gad.12.7.956](#)
28. G. J. Beitel, M. A. Krasnow, Genetic control of epithelial tube size in the *Drosophila* tracheal system. *Development* **127**, 3271–3282 (2000). [Medline](#)

29. S. J. Marygold, P. C. Leyland, R. L. Seal, J. L. Goodman, J. Thurmond, V. B. Strelets, R. J. Wilson; FlyBase consortium, FlyBase: Improvements to the bibliography. *Nucleic Acids Res.* **41**, D751–D757 (2013). [Medline doi:10.1093/nar/gks1024](#)
30. G. Dietzl, D. Chen, F. Schnorrer, K. C. Su, Y. Barinova, M. Fellner, B. Gasser, K. Kinsey, S. Oettel, S. Scheiblauer, A. Couto, V. Marra, K. Keleman, B. J. Dickson, A genome-wide transgenic RNAi library for conditional gene inactivation in *Drosophila*. *Nature* **448**, 151–156 (2007). [Medline doi:10.1038/nature05954](#)
31. D. Sutherland, thesis, Stanford University (1999).
32. K. G. Golic, S. Lindquist, The FLP recombinase of yeast catalyzes site-specific recombination in the *Drosophila* genome. *Cell* **59**, 499–509 (1989). [Medline doi:10.1016/0092-8674\(89\)90033-0](#)
33. K. Certel, M. G. Anderson, R. J. Shrigley, W. A. Johnson, Distinct variant DNA-binding sites determine cell-specific autoregulated expression of the *Drosophila* POU domain transcription factor *drifter* in midline glia or trachea. *Mol. Cell. Biol.* **16**, 1813–1823 (1996). [Medline](#)
34. K. Ito, W. Awano, K. Suzuki, Y. Hiromi, D. Yamamoto, The *Drosophila* mushroom body is a quadruple structure of clonal units each of which contains a virtually identical set of neurones and glial cells. *Development* **124**, 761–771 (1997). [Medline](#)
35. J. Huang, W. Zhou, W. Dong, A. M. Watson, Y. Hong, Directed, efficient, and versatile modifications of the *Drosophila* genome by genomic engineering. *Proc. Natl. Acad. Sci. U.S.A.* **106**, 8284–8289 (2009). [Medline doi:10.1073/pnas.0900641106](#)
36. M. G. Anderson, G. L. Perkins, P. Chittick, R. J. Shrigley, W. A. Johnson, *drifter*, a *Drosophila* POU-domain transcription factor, is required for correct differentiation and migration of tracheal cells and midline glia. *Genes Dev.* **9**, 123–137 (1995). [Medline doi:10.1101/gad.9.1.123](#)
37. M. Ashburner, K. G. Golic, R. S. Hawley, *Drosophila: A Laboratory Handbook* (Cold Spring Harbor Laboratory Press, Cold Spring Harbor, NY, ed. 2, 2005).
38. B. P. Levi, A. S. Ghabrial, M. A. Krasnow, *Drosophila* talin and integrin genes are required for maintenance of tracheal terminal branches and luminal organization. *Development* **133**, 2383–2393 (2006). [Medline doi:10.1242/dev.02404](#)
39. N. Hacohen, S. Kramer, D. Sutherland, Y. Hiromi, M. A. Krasnow, *sprouty* encodes a novel antagonist of FGF signaling that patterns apical branching of the *Drosophila* airways. *Cell* **92**, 253–263 (1998). [Medline doi:10.1016/S0092-8674\(00\)80919-8](#)